Progress in Organic Coatings 147 (2020) 105737

Contents lists available at ScienceDirect

Progress in Organic Coatings

journal homepage: www.elsevier.com/locate/porgcoat

Design and preparation of icephobic PDMS-based coatings by introducing an aqueous lubricating layer and macro-crack initiators at the ice-substrate interface

Zhiwei He[a,b], Yizhi Zhuo[b], Feng Wang[b], Jianying He[b], Zhiliang Zhang[b,*]

[a] College of Materials and Environmental Engineering, Hangzhou Dianzi University, Hangzhou 310018, China
[b] NTNU Nanomechanical Lab, Department of Structural Engineering, Norwegian University of Science and Technology (NTNU), Trondheim 7491, Norway

ARTICLE INFO

Keywords:
Anti-icing
Ice adhesion strength
Aqueous lubricating layer
Macro-crack initiator
Macro-scale hollow sub-surface structures

ABSTRACT

Preventing ice accretion on exposed surfaces is important to the operational performance of various facilities and devices. As time elapses and temperature lowers sufficiently, ice accretion becomes inevitable. Herein, we present a new approach to prepare icephobic coatings by incorporating two strategies towards lowering ice adhesion strength, i.e. introducing an aqueous lubricating layer and maximizing macro-crack initiators at the ice-substrate interface. The aqueous lubricating layer is realized by grafting poly(acrylic acid) (PAA) onto polydimethylsiloxane (PDMS) coatings, and the macro-crack initiators are induced by introducing macro-scale hollow sub-surface structures into PDMS coatings. By using vertical shear tests, ice adhesion strengths of PAA-*g*-PDMS (10:1), PDMS coatings with macro-scale hollow sub-surface structures (hPDMS) (10:1), PAA-*g*-hPDMS (10:1), PAA-*g*-PDMS (10:10), hPDMS (10:10), and PAA-*g*-hPDMS (10:10) coatings are obtained as 178.5 ± 22 kPa, 153.1 ± 19 kPa, 122.7 ± 18 kPa, 24.6 ± 4 kPa, 20.3 ± 3.4 kPa and 17.6 ± 3.2 kPa, respectively, showing a reduction of 37.2 %, 46.1 %, 56.8 %, 32.8 %, 44.5 % and 51.9 % when compared with corresponding pure PDMS coatings. These results indicate that ice adhesion strength can be further reduced by simultaneously introducing two strategies. The principle of designing icephobic coatings by combining two or more strategies to reduce ice adhesion to as low as possible provides a new avenue to the preparation of icephobic coatings, and makes practical applications possible under extremely severe conditions.

1. Introduction

Preventing ice accretion on exposed surfaces is important to the operational performance of various facilities and devices, such as power lines, vehicles, aircrafts, wind turbines, and oil drilling rigs [1–3]. To reduce risks caused by ice accretion, both active and passive methods have been developed. Active strategies, such as de-icing fluid spray and thermal heating, induce high costs and energy demands as well as potential environmental pollutions and safety concerns. Compared with active approaches, passive icephobic coatings without external energy input are preferred, which are supposed to repel incoming water droplets, suppress ice nucleation and/or lower ice adhesion strength [3–6].

As time elapses and temperature lowers sufficiently, icing becomes inevitable on exposed surfaces. One practical solution to achieve surface icephobicity is to lower ice adhesion to as low as possible [3]. Recently, there are various strategies proposed towards the design of icephobic surfaces by lowering ice adhesion, as shown in Fig. 1, including (super-)hydrophobic surfaces [7–14], polyelectrolyte polymer brushes [15–17], aqueous lubricating layers [18–25], organic lubricating layers [26–30], low elastic modulus surfaces [31–36], and multi-scale crack initiator-promoted icephobic surfaces [3–5,37,38]. For example, low surface energy of (super-)hydrophobic surfaces and potential micro-scale cracks at ice-substrate interface contribute to the reduction of ice adhesion strength during a de-icing test. The polyelectrolyte polymer brushes usually contain a hydrophilic regime and a hydrophobic regime, and ice adhesion strength can be varied by changing the hydration state of these brushes. For aqueous lubricating layers, a non-frozen liquid-like water layer can exist at ice-substrate interface, which works as a lubricating layer and thus reduce the ice adhesion strength. Organic lubricating layers can serve as a sacrificial layer during icing/de-icing cycles and therefore possess low ice adhesion strength. The deformation incompatibility can occur between low elastic modulus surfaces and ice, which is beneficial to the reduction of ice adhesion strength. Moreover, multi-scale crack initiator-promoted

* Corresponding author.
E-mail address: zhiliang.zhang@ntnu.no (Z. Zhang).

https://doi.org/10.1016/j.porgcoat.2020.105737
Received 12 November 2019; Received in revised form 3 April 2020; Accepted 28 April 2020

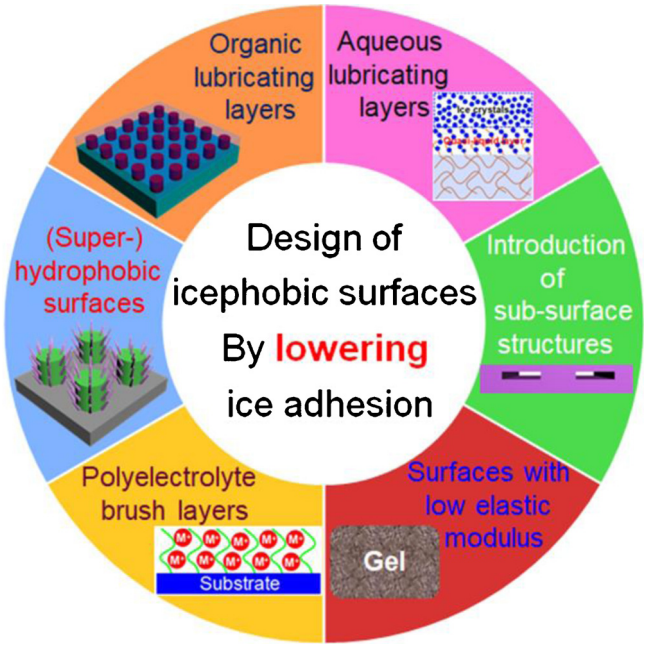

Fig. 1. Strategies towards design of icephobic surfaces by lowering ice adhesion strength.

icephobic surfaces show low ice adhesion strength due to the formation of multi-scale cracks during a de-icing test. Although these strategies have their particular de-icing mechanisms, they may reach the limitation of lowering ice adhesion when working individually. To achieve ice adhesion strength as low as possible, it is worthy of combining two or more above strategies when designing new types of icephobic coatings.

For example, Golovin et al. prepared organic lubricating layers by adding oils into low elastic modulus substrates to obtain icephobic coatings [39,40]. Wang et al. reported robust anti-icing surfaces by combining superhydrophobic surfaces and low elastic modulus substrates [41]. He et al. induced macro-cracks at the ice-substrate interface by introducing macro-scale hollow sub-surface structures into low elastic modulus substrates to obtain super-low ice adhesion surfaces [3–5]. The above icephobic coatings combine the strategy of low elastic modulus with other strategies (e.g., organic lubricating layer, superhydrophobic surface, and macro-crack promoted surface), showing excellent icephobicity of multiple strategies designed icephobic coatings [42]. Similarly, it is also possible to combine multi-scale cracks promoted surfaces with other strategies, such as aqueous lubricating layers, low elastic modulus surfaces and superhydrophobic surfaces [3,4]. However, multiple strategies designed icephobic coatings have not received attention, which are worthy of being discussed so that new types of icephobic coating can be utilized in different conditions.

The aqueous water layer can exist at the ice-substrate interface below 0 °C and thus serves as a lubricating layer during a de-icing test [43,44]. Generally, this non-frozen liquid-like water layer can be realized by grafting hygroscopic molecules or polymers and then forming hydrophilic surfaces. For example, Chen et al. designed self-lubricating icephobic coatings by blending polydimethylsiloxane (PDMS)-poly (ethylene glycol) (PEG) amphiphilic copolymers into a polymer coating matrix [18]. Chen et al. constructed a self-sustainable lubricating layer by modifying solid substrates with highly hydrophilic poly(acrylic acid) – dopamine, and then obtained anti-icing coatings with low ice adhesion [45]. Ozbay et al. prepared aqueous lubricating layers by introducing hydrophilic lubricants (e.g., water, ethylene glycol, formamide, and water-glycerine mixture) to filter papers and polypropylene-sorbent sheets [46]. Li et al. obtained highly transparent antifogging/anti-icing coatings from amphiphilic block copolymers [47]. Wang et al. designed and prepared various anti-icing coatings with aqueous lubricating layers inspired by ice skating [19]. They introduced the hyaluronic acid [19], dimethylolpropionic acid [48] and poly(acrylic acid) [20] as the hydrophilic components to realize an aqueous lubricating layer to achieve surface icephobicity. In addition to the above studies, the combination of an aqueous lubricating layer with other strategies towards design of icephobic coatings has rarely been studied.

Multi-scale crack initiator-promoted icephobic surfaces have been investigated in recent years [3]. From the viewpoint of fracture mechanics, the purpose of this strategy is to create multi-scale crack initiators at the ice-substrate interface such that ice adhesion can be largely reduced. For example, Nosonovsky et al. reported that ice adhesion strength depends on the receding contact angle and the initial size of interfacial cracks [49]. Ling et al. reported that the formation of micro-cracks acts as interfacial stress concentrators and thus reduces ice adhesion [37]. Chen et al. utilized a swelling force to create cracks at the ice-substrate interface and thus decreased ice adhesion [38]. He et al. found that macro-crack initiator-promoted icephobic surfaces can reduce ice adhesion down to 5.7 kPa without using any slippery agents due to the introduction of macro-scale hollow sub-surface structures [3], and then they investigated the role of macro-scale hollow subsurface structures in reducing ice adhesion [5]. He et al. also reported sandwich-like PDMS sponge-based surfaces with super-low ice adhesion (~1 kPa) which was achieved by incorporating macro-cracks, low elastic modulus and a top smooth layer [4]. The key of this strategy is to maximize the total length of cracks and achieve ductile fracture at the ice-substrate interface, and thus to obtain the lowest ice adhesion possible.

Herein, we design and fabricate poly(acrylic acid) (PAA) grafted PDMS-based icephobic coatings by simultaneously introducing an aqueous lubricating layer and macro-crack initiators at the ice-substrate interface. To lower ice adhesion strength, these two strategies can separately achieve a reduction of 37.2 % and 46.1 % for PDMS (10:1) based coatings and a reduction of 32.8 % and 44.5 % for PDMS (10:10) based coatings when compared with corresponding pure PDMS coatings, and the combination of these two strategies can even reach a reduction of 56.8 % and 51.9 %, respectively. This approach provides a new insight into the design of icephobic coatings with low ice adhesion strength.

2. Materials and methods

2.1. Chemical materials

The Sylgard®184 silicone elastomer kit was purchased from Dow Corning Corporation. 3-(trimethoxysilyl)propyl methacrylate (TPM, 98 %), acetic acid (≥99.7 %), isopropyl alcohol (≥98 %), ethanol (≥99.5 %), acetone (≥99.5 %), acrylic acid (99 %) and 2-hydroxy-2-methylpropiophenone (97 %) were purchased from Sigma Aldrich. All reagents were used as received.

2.2. Preparation of SU8 patterns

The SU-8 5 (MicroChem Corp., Newton, MA) photoresist was used to fabricate SU-8 pillar pattern on silicon wafer via a photolithography process [3]. The edge-to-edge spacing was 1 mm. The speed of spin-coating (WS-400B-6NPP-LITE/AS, Laurell Technologies) was selected at 3000 rpm to obtain the SU-8 pillar pattern with a height of 5 μm. The dimension of a SU-8 pillar was 1 mm × 1 mm × 5 μm.

2.3. Preparation of hPDMS

The preparation process of PDMS coatings with macro-scale hollow sub-surface structures (hPDMS) is described in Fig. 2a, based on but improved from our previous study [3]. First, a silicone base and a

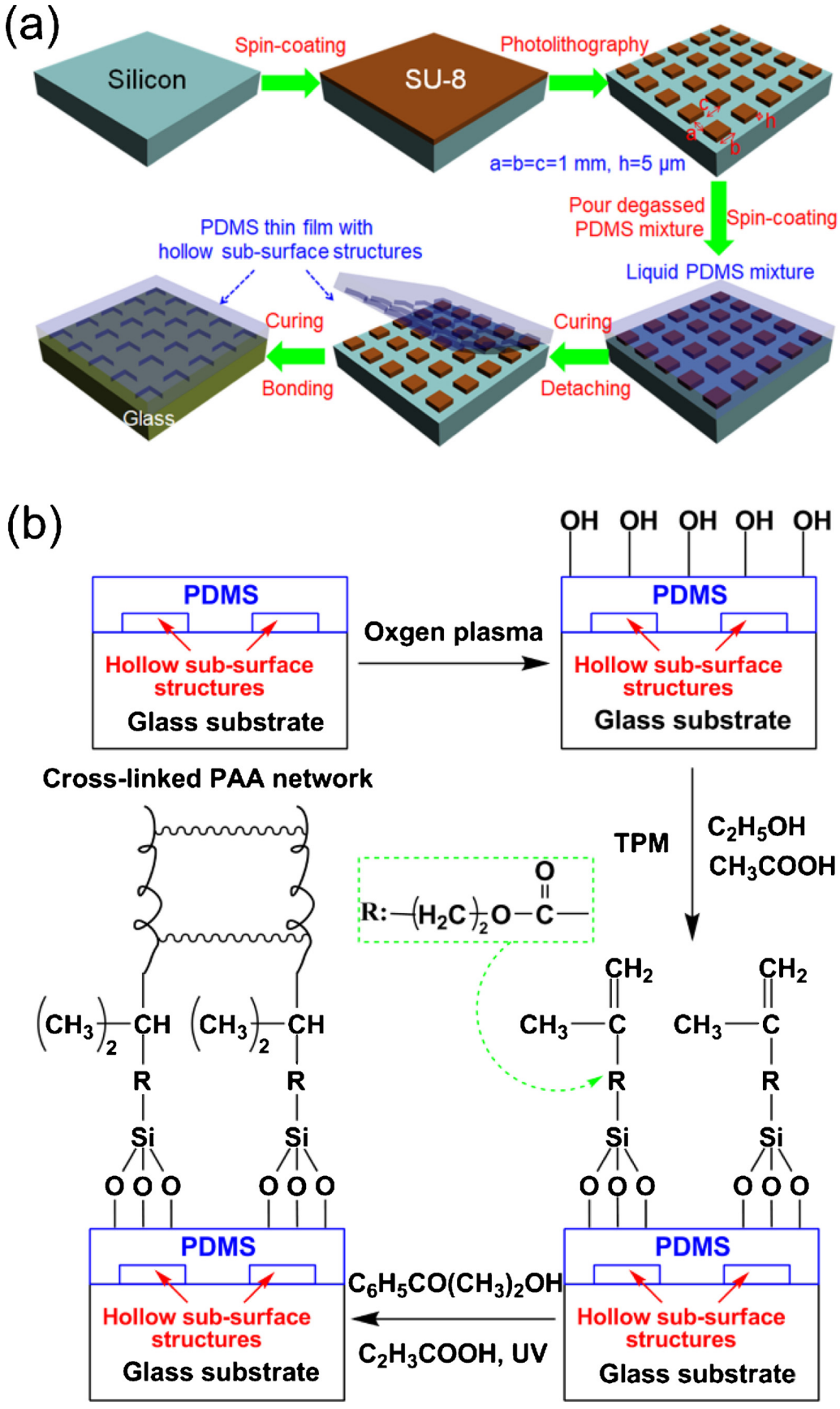

Fig. 2. The fabrication routes of (a) hPDMS coatings and (b) PAA-*g*-hPDMS coatings.

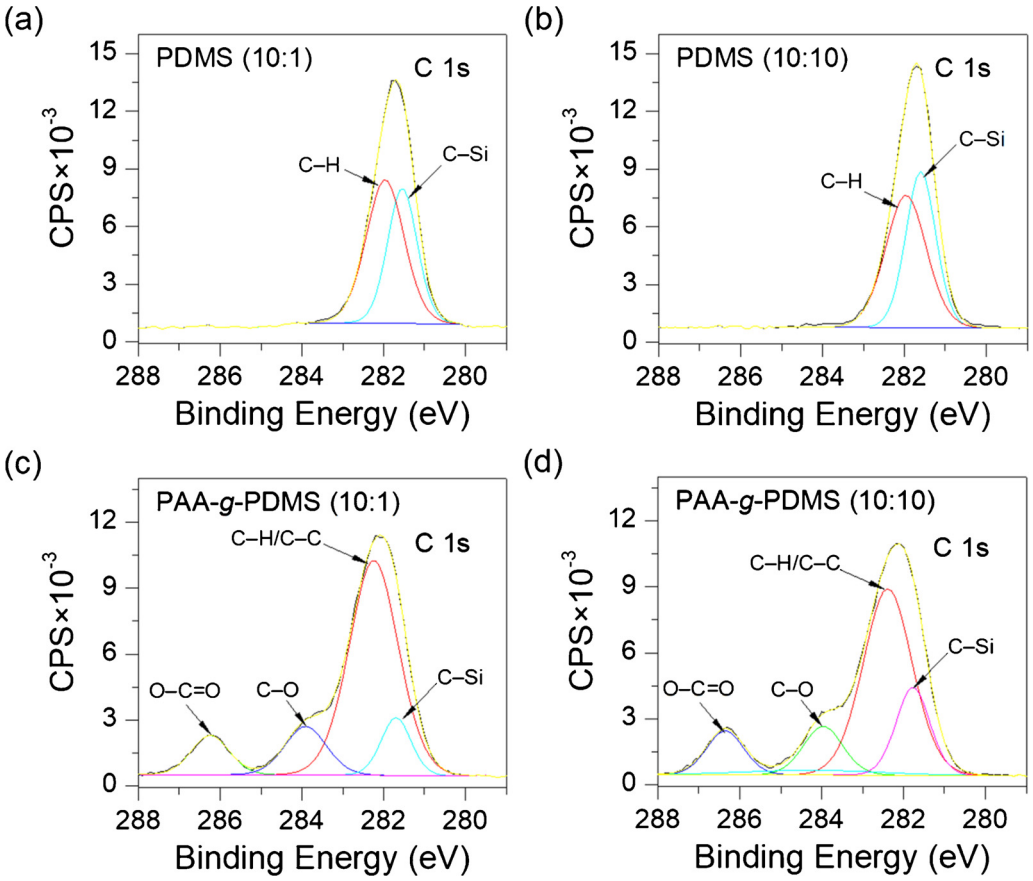

Fig. 3. XPS C 1s spectra of (a) PDMS (10:1), (b) PDMS (10:10), (c) PAA-*g*-PDMS (10:1), and (d) PAA-*g*-PDMS (10:10).

curing agent of Sylgard®184 in different weight ratios (10:1 and 10:10) were mixed, stirred vigorously, and degassed to remove air bubbles. The above liquid mixture was poured on a SU-8 patterned silicon wafer and was spin-coated for 30 s with a speed of 1400 rpm to obtain PDMS coatings with a thickness of 67 μm after a curing process (65 ˚C, 2 h). Both glass substrates and PDMS coatings were treated with oxygen plasma (Femto plasma cleaner, 50 % O_2 flow/80 % power) for 12 s. Then the PDMS coating was peeled off from the silicon wafer and coated on the glass substrate, followed by curing the PDMS coating for another 2 h at 65 ˚C. Finally, the hPDMS coatings were obtained.

2.4. Preparation of PAA-g-PDMS coatings

The grafting of PAA onto PDMS coatings is described in Fig. 2b, improved from previous studies [20,50]. First, the PDMS coating was treated by oxygen plasma for 30 s, reacted with a TPM solution (50 % v/v TPM and 0.1 % v/v acetic acid in pure ethanol) within 15 min, and heated at 120 ˚C for 5 min. Then, the obtained PDMS coating was washed by isopropyl alcohol and ethanol, followed by drying and curing at 65 ˚C for 2 h and 30 min. In the subsequent step, the PDMS coating was immersed in a monomer solution (20 % acrylic acid and 5% 2-hydroxy-2-methylpropiophenone) under the irradiation of UV (UV zone cleaner) for 15 min, at 72 mW cm^{-2}, producing covalent linkages between the acrylate group of acrylic acid and the methacrylate group of TPM. Finally, the hydrophilic PAA-*g*-PDMS coating was obtained after thoroughly washing by de-ionized water.

2.5. Characterization

The surface roughness of PDMS-based coatings was characterized by using a profilometer (Dektak 150, Veeco) equipped with a 12.5 μm diamond tip stylus. The water contact angle was evaluated by using a CAM 200 contact-angle system (KSV Instruments Ltd., Helsinki, Finland). The receding contact angle (θ_{rec}) was tested and repeated for 5 times, where water was supplied via a syringe in or out of sessile droplets (~5 μL) [2]. The water adhesion force was investigated by a Dynamic Contact Angle Tensiometer (DCAT11®, dataphysics) and repeated for 10 times [2]. Chemical structures of PDMS and PAA-*g*-PDMS coatings were examined by X-ray photoelectron spectroscopy (XPS, Kratos Axis Ultra DLD).

2.6. Ice adhesion strength

The ice adhesion strength was measured by a vertical shear test (Instron MicroTester, Instron® Model 5944), following the same procedure as described in previous studies [3–5,29–31]. The details of freezing behavior of samples were as follows: 10 mL de-ionized water was filled in a polypropylene centrifuge tube mold sealed on PDMS coatings by using a silicone sealant (Loctite ®5926), followed by keeping the system in a refrigerator at −18 ˚C for 2 ~ 24 h [3–5]. Then the system was rapidly transported from the refrigerator to a cooling chamber (−18 ˚C) where the system was stabilized at −18 ˚C for 30 min. A force probe with a diameter of 5 mm was used to propel the tube-encased ice columns at a velocity of 0.1 mm min^{-1} during an ice adhesion test. Each sample was tested for three times, and the standard error was used for the tested data. For the icing/de-icing cyclic tests, the freezing time was chosen as 2 h to save time, for it has been demonstrated that the freezing time (2 ~ 24 h) of water had no significant effect on the values of ice adhesion strength [4,32].

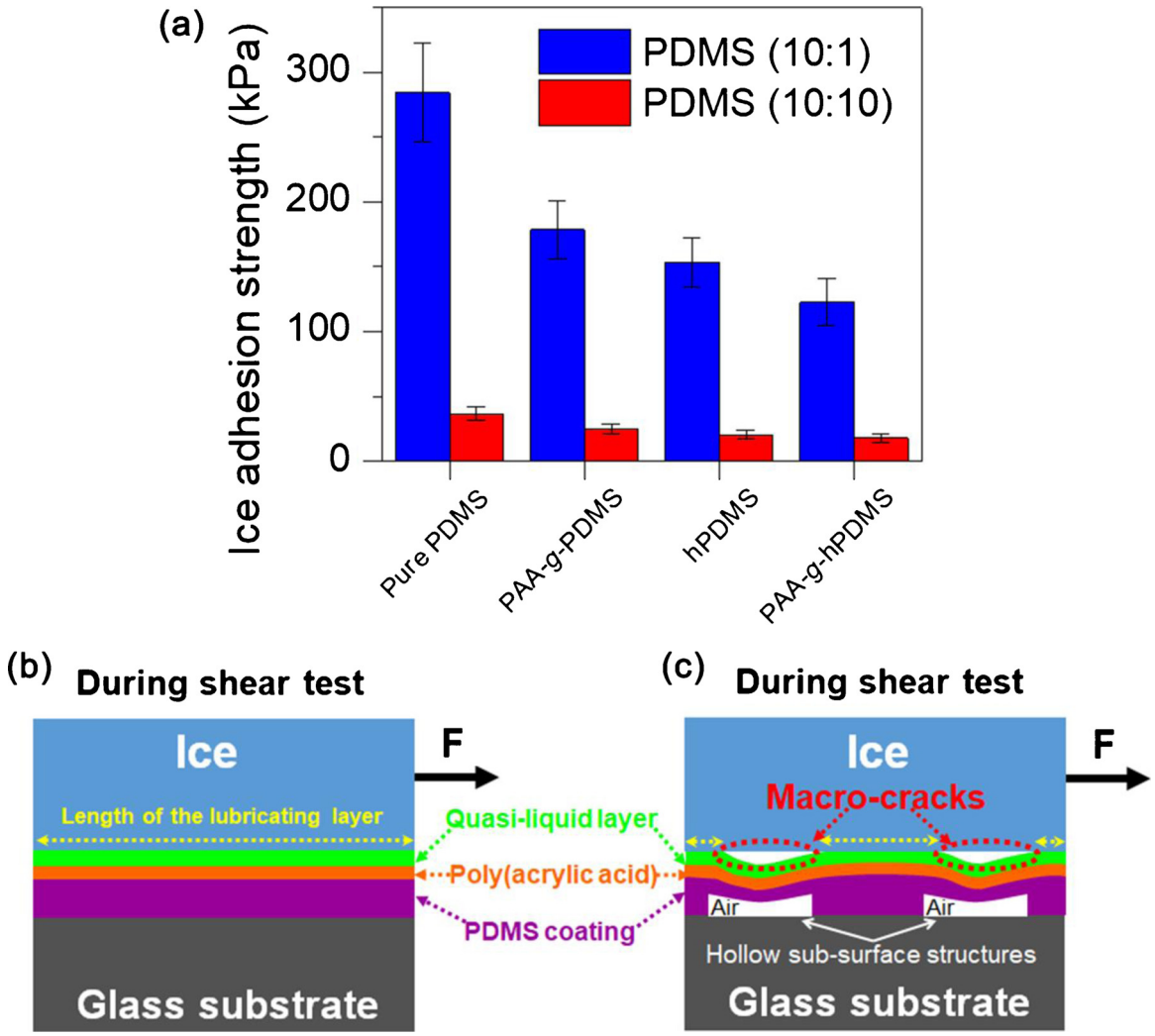

Fig. 4. (a) Ice adhesion strength of eight PDMS-based coatings, (b) De-icing mechanism of an aqueous lubricating layer, (c) De-icing mechanism of the combination of an aqueous lubricating layer and macro-scale hollow sub-surface structures.

3. Results and discussion

3.1. X-ray photoelectron spectroscopy

To have a better understanding of the surface chemistry of PDMS, hPDMS, PAA-*g*-PDMS and PAA-*g*-hPDMS coatings, X-ray photoelectron spectroscopy (XPS) analysis of PDMS and PAA-*g*-PDMS is performed, as shown in Fig. 3 and Fig. S1-S3. For hPDMS and PAA-*g*-hPDMS coatings, macro-scale hollow sub-surface structures will not influence the surface chemistry. The XPS analysis indicates that PDMS-based coatings contain elements of oxygen, carbon and silicon (Fig. S1). The spectrum is shifted to fix the C − C/C–H peak at 284.6 eV because of possible surface charging of PDMS coatings [51]. For example, peak fitted C 1s spectra of PDMS (10:1), PDMS (10:10), PAA-*g*-PDMS (10:1) and PAA-*g*-PDMS (10:10) coatings are shown in Fig. 3. For PDMS (10:1 or 10:10) coatings, the peaks of C − C/C–H and C − Si are 284.6 eV and 284.2 eV (Fig. 3a and b) [52]. It is found that the relative intensity of C − C/C–H to C − Si for PDMS (10:10) is weaker than that of PDMS (10:1) because of less components of base materials as shown in the polymerization process (Fig. S4). When the PAA is grafted onto PDMS coatings, the binding energy at 288.9 eV and 286.5 eV belongs to O − C=O and C − O [53]. The relative intensity of C − C/C–H to C − Si for PAA-*g*-PDMS (10:10) is weaker than that of PAA-*g*-PDMS (10:1), which is in agreement with the above results in Fig. 3a and b. In short, different surface chemistry can cause different surface energy, and thus influence ice adhesion strength of four PDMS-based coatings.

3.2. Ice adhesion strength

Ice adhesion strengths of PDMS-based coatings with a thickness of 67 μm have been measured by a vertical shear test (see the experimental section), and the results are shown in Fig. 4a. The PDMS coatings with macro-scale hollow sub-surface structures and the PAA-*g*-PDMS coatings with macro-scale hollow sub-surface structures are labeled as hPDMS and PAA-*g*-hPDMS, respectively. For pure PDMS (10:1) coatings, ice adhesion strength is 284.2 ± 38 kPa. When the aqueous lubricating layer is introduced into pure PDMS (10:1) coatings, ice adhesion strength of PAA-*g*-PDMS (10:1) coatings is 178.5 ± 22 kPa, showing a reduction of 37.2 % for ice adhesion because of the existence of a liquid-like water layer at the ice-substrate interface as several studies reported [18–20,48]. If macro-scale hollow sub-surface structures are introduced

into pure PDMS (10:1) coatings, ice adhesion strength of hPDMS coatings is reduced to 153.1 ± 19 kPa and shows a reduction for ice adhesion as 46.1 %, which is caused by the occurrence of macro-crack initiators at the ice-substrate interface during a shear test.

When designing icephobic coatings by incorporating two strategies (the aqueous lubricating layer and macro-scale hollow sub-surface structures), the results of ice adhesion strength are also shown in Fig. 4a. The ice adhesion strength of PAA-*g*-hPDMS (10:1) coatings is

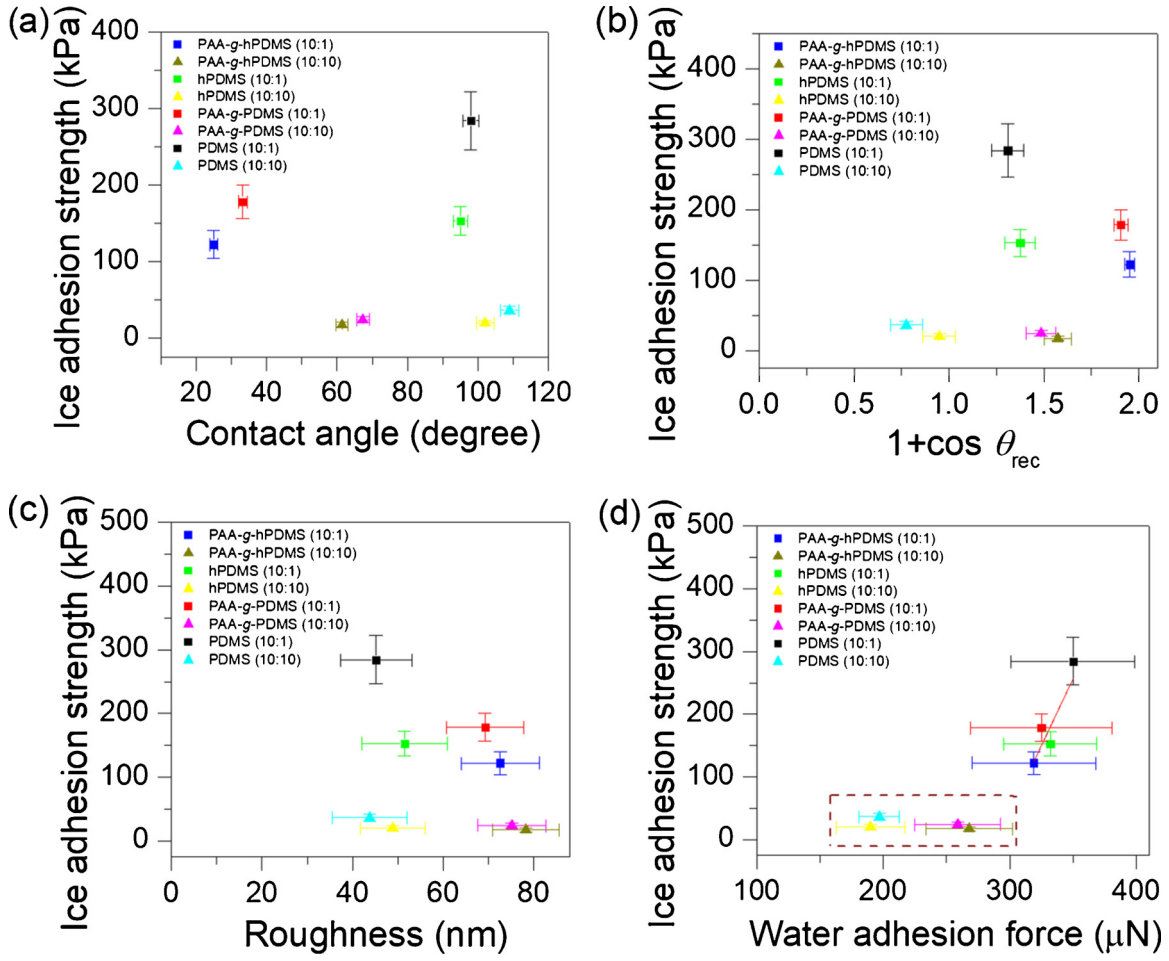

Fig. 5. Room temperature characteristics of PDMS-based coatings.

122.7 ± 18 kPa and reaches a reduction of 56.8 %. The de-icing mechanisms of two strategies are schematically illustrated in Fig. 4b and c. For PAA-*g*-PDMS coatings, the reduction of ice adhesion strength is caused by the lubricating function of the aqueous lubricating layer, and the whole lubricating layer is effective for the reduction of ice adhesion strength. For hPDMS coatings, ice adhesion strength is largely reduced due to the introduction of macro-crack initiators (Fig. 4c), which causes stiffness inhomogeneity in both perpendicular and tangential directions to weaken the ice–solid interface and maximizes the crack length underneath the ice [3].

Tuning the weight ratio of base material and curing agent is another approach that can change elastic modulus and surface energy of PDMS substrates [3,4]. As shown in Fig. 4a, when the weight ratio of PDMS prepolymer and curing agent is changed from 10:1 to 10:10, ice adhesion strengths of pure PDMS, PAA-*g*-PDMS, hPDMS and PAA-*g*-hPDMS are 36.6 ± 5.4 kPa, 24.6 ± 4 kPa, 20.3 ± 3.4 kPa and 17.6 ± 3.2 kPa, respectively. The reductions of ice adhesion strength for PAA-*g*-PDMS (10:10), hPDMS (10:10) and PAA-*g*-hPDMS (10:10) are 32.8 %, 44.5 % and 51.9 % when compared with pure PDMS (10:10) coatings, respectively. It can be seen from the above results that ice adhesion strength can be reduced by decreasing the weight ratio of base material and curing agent. Lower weight ratio of base material and curing agent can result in lower elastic modulus of PDMS coatings, and thus leads to lower ice adhesion strength of PDMS coatings [4]. Moreover, the combination of two strategies still works for the further reduction of ice adhesion strength of PDMS (10:10) coatings when compared with individual strategy. This indicates that the incorporation of two strategies (the aqueous lubricating layer and macro-scale hollow sub-surface structures) may be proper for the design of icephobic PDMS-based coatings with different weight ratios.

3.3. Relationships between room temperature characteristics and ice adhesion strength

The characterization of ice adhesion strength is a direct method to evaluate surface icephobicity. However, ice adhesion tests require low temperature operation, which is costly and time-consuming. To facilitate the evaluation of surface icephobicity, it is interesting to correlate ice adhesion strength with room temperature characteristics of coatings. Herein, the correlations between room temperature characteristics (e.g., surface wettability, roughness and water adhesion force) and ice adhesion strength are investigated and plotted in Fig. 5.

It can be seen from Fig. 5a that water contact angle has no obvious correlation with ice adhesion strength of the prepared PDMS-based coatings [4,18]. This is because water contact angle only reflects the surface chemistry and topography, while ice adhesion strength is determined by various parameters, such as surface chemistry and topography, elastic modulus, the aqueous lubricating layer, macro-cracks at the ice-substrate interface, and so on [3,4,18]. Generally, the increase of contact angle and the decrease of surface energy are favorable to the reduction of ice adhesion strength [54,55]. In this study, the grafting of hydrophilic PAA onto PDMS coatings not only lowers water contact angle, but also leads to the reduction of ice adhesion strength by introducing an interfacial non-frozen water layer [18]. Compared with PDMS (10:1) coatings, PDMS (10:10) coatings have higher water contact angle and lower ice adhesion strength because of lower surface energy and elastic modulus. For PDMS and hPDMS coatings, both have similar water contact angle, but ice adhesion strength of hPDMS

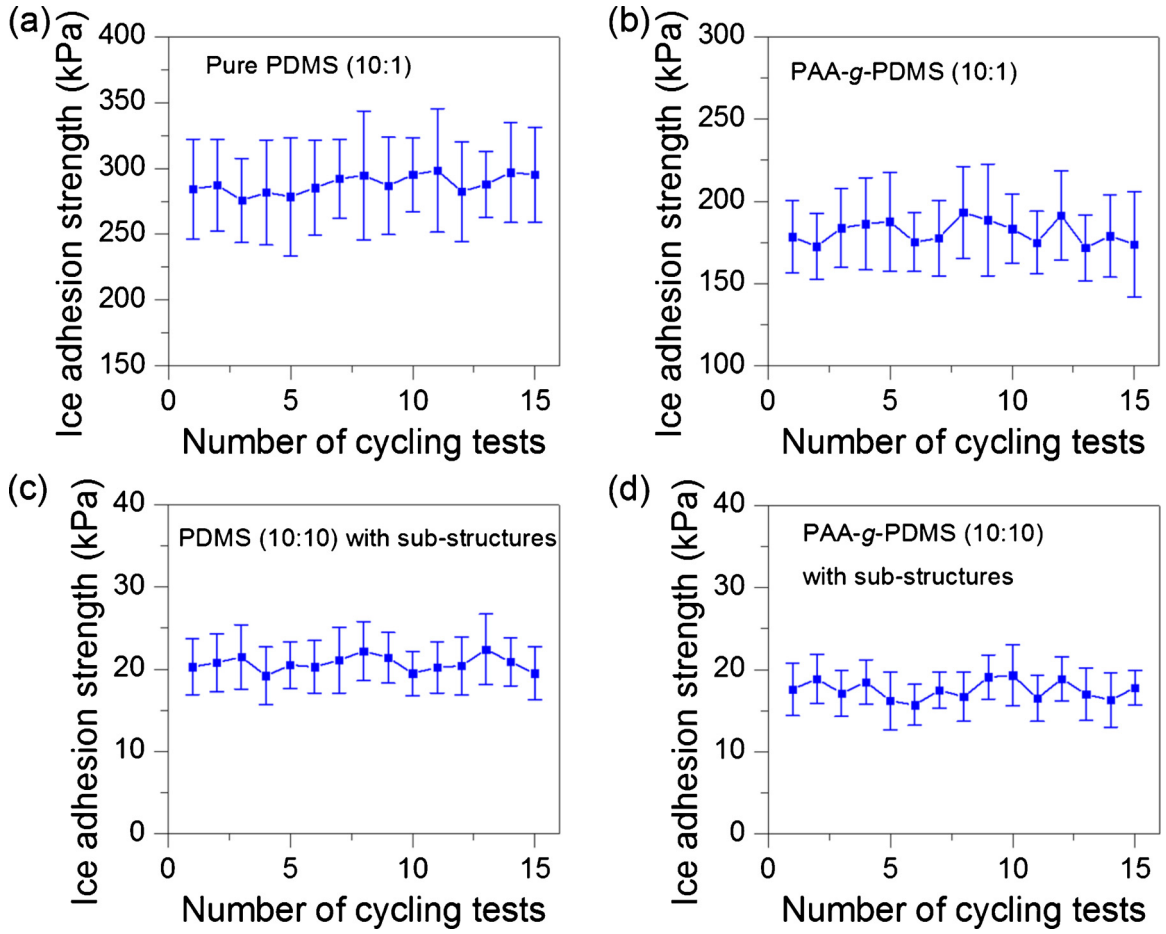

Fig. 6. Icing/de-icing cycling tests of (a) pure PDMS (10:1), (b) PAA-g-PDMS (10:1), (c) hPDMS (10:10), (d) PAA-*g*-hPDMS (10:10).

coatings is lower than that of PDMS coatings. Because the measurement of water contact angle cannot reveal the role of the macro-scale hollow sub-surface structures, while it significantly contributes to the reduction of ice adhesion strength by inducing macro-cracks at the ice-substrate interface [3]. Similarly, the value of $[1 + \cos \theta_{rec}]$ is not proper to correlate with ice adhesion strength of low elastic coatings with or without macro-scale hollow sub-surface structures (Fig. 5b), in agreement with early work by Chen et al. [18] and He et al. [4].

As for the root-mean-square roughness (R_q), it ranges from 35 to 85 nm for the eight PDMS-based coatings (Fig. 5c). The roughness of PDMS (10:1) and PDMS (10:10) coatings is almost the same, while ice adhesion strength of PDMS (10:1) coatings is about 7 times as that of PDMS (10:10) coatings. Therefore, surface roughness cannot individually dictate ice adhesion strength [2]. Furthermore, the correlation between water adhesion force and ice adhesion strength is shown in Fig. 5d. It can be found that water adhesion forces on PDMS-based coatings (10:10) are lower than that of corresponding PDMS-based coatings (10:1), indicating the influence of elastic modulus on ice adhesion strength. Similarly, hPDMS coatings with lower water adhesion forces show lower ice adhesion strength for the corresponding PDMS coatings with same weight ratios. When ice adhesion strength is larger than 100 kPa, a linear relationship can be obtained with the square of the correlation coefficient ($R^2 = 0.60$). When ice adhesion strength is less than 60 kPa, water adhesion force is in a range from 160 to 315 μN, which is in agreement with previous studies [2,4]. Although ice adhesion strength cannot be precisely predicted by water adhesion force in the above range, it can be estimated whether it is above or below 60 kPa if we know exact values of water adhesion forces as suggested by our previous studies [2,4]. In short, it is cost-effective to estimate ice adhesion strength of unknown coatings by some room temperature characteristics (e.g., water adhesion force).

3.4. Icing/de-icing cycling tests

The surface durability is an important parameter that evaluates the long-term performance of icephobic coatings in real applications. In Fig. 6, the icing/de-icing cyclic testing results of four selected PDMS-based coatings are presented. In all icing/de-icing cyclic tests, the freezing time in icing/de-icing cyclic tests was chosen as 2 h [4,32], because the freezing time (2 ~ 24 h) of water had no significant effect on the values of ice adhesion strength as demonstrated by Beemer et al. and He et al. For the failure of ice, the detachment of ice on PDMS-based coatings has been confirmed as the adhesive failure. Over 15 cyclic tests, ice adhesion strengths of pure PDMS (10:1), PAA-*g*-PDMS (10:1), hPDMS (10:10) and PAA-*g*-hPDMS (10:10) coatings are stable around 281 kPa, 180 kPa, 21 kPa and 17 kPa, respectively. It indicates the durability of the prepared PDMS-based coatings is fitted for a long-term use as our previous studies and other reports suggested [3,4,32,34,39,40]. For organic lubricating coatings, the depletion of organic lubricants needs to be considered [56], while the stability of hollow sub-surface structures of PAA-*g*-hPDMS coatings should be concerned for a long-term use. Besides, other factors, such as abrasion, corrosion and UV resistances, also need to be considered when applying these coatings in real applications.

4. Conclusions

We present a new approach to prepare icephobic coatings by combining two strategies towards lowering ice adhesion, i.e. introducing an aqueous lubricating layer and maximizing macro-crack initiators at the

ice-substrate interface. The reductions of ice adhesion strength for PAA-*g*-hPDMS (10:1) and PAA-*g*-hPDMS (10:10) are 56.8 % and 51.9 % when compared with corresponding pure PDMS coatings, respectively. These results indicate that the combination of two strategies can further reduce ice adhesion strength for PDMS coatings with different weight ratios. We envision that strategies, such as an aqueous lubricating layer and macro-crack initiators induced by macro-scale hollow sub-surface structures, can be used to combine with other strategies, which opens a new avenue to the design of icephobic coatings.

Declaration of Competing Interest

All authors declare no conflict of interest.

Acknowledgements

The Research Council of Norway is acknowledged for the support to the FRINATEK project Towards Design of Super-Low Ice Adhesion Surfaces (SLICE, 250990), the PETROMAKS2 project Durable Arctic Icephobic Materials (AIM, 255507), and the support to the Norwegian Micro- and Nano-Fabrication Facility, NorFab (245963/F50). The National Natural Science Foundation of China (Grant No. 51803043) and the Science Foundation of Hangzhou Dianzi University (KYS205618119) are appreciated for the financial support.

Appendix A. Supplementary data

Supplementary material related to this article can be found, in the online version, at doi:https://doi.org/10.1016/j.porgcoat.2020.105737.

References

[1] A.J. Meuler, J.D. Smith, K.K. Varanasi, J.M. Mabry, G.H. McKinley, R.E. Cohen, Relationships between water wettability and ice adhesion, ACS Appl. Mater. Interfaces 2 (2010) 3100–3110.
[2] Z. He, E.T. Vågenes, C. Delabahan, J. He, Z. Zhang, Room temperature characteristics of polymer-based low ice adhesion surfaces, Sci. Rep. 7 (2017) 42181.
[3] Z. He, S. Xiao, H. Gao, J. He, Z. Zhang, Multiscale crack initiator promoted super-low ice adhesion surfaces, Soft Matter 13 (2017) 6562–6568.
[4] Z. He, Y. Zhuo, J. He, Z. Zhang, Design and preparation of sandwich-like PDMS sponges with super-low ice adhesion, Soft Matter 14 (2018) 4846–4851.
[5] Z. He, Y. Zhuo, F. Wang, J. He, Z. Zhang, Understanding the role of hollow sub-surface structures in reducing ice adhesion strength, Soft Matter 15 (2019) 2905–2910.
[6] V. Hejazi, K. Sobolev, M. Nosonovsky, From superhydrophobicity to icephobicity: forces and interaction analysis, Sci. Rep. 3 (2013) 2194.
[7] Z. He, Z. Zhang, J. He, CuO/Cu based superhydrophobic and self-cleaning surfaces, Scripta Mater. 118 (2016) 60–64.
[8] Z. He, J. He, Z. Zhang, Selective growth of metallic nanostructures on micro-structured copper substrate in solution, CrystEngComm 17 (2015) 7262–7269.
[9] T. Jing, Y. Kim, S. Lee, D. Kim, J. Kim, W. Hwang, Frosting and defrosting on rigid superhydrohobic surface, Appl. Surf. Sci. 276 (2013) 37–42.
[10] M.M. Ahmad, A. Eshaghi, Fabrication of antireflective superhydrophobic thin film based on the TMMS with self-cleaning and anti-icing properties, Prog. Org. Coat. 122 (2018) 199–206.
[11] K.R. Khedir, G.K. Kannarpady, C. Ryerson, A.S. Biris, An outlook on tunable superhydrophobic nanostructural surfaces and their possible impact on ice mitigation, Prog. Org. Coat. 112 (2017) 304–318.
[12] H. Zhang, X. Lu, Z. Xin, W. Zhang, C. Zhou, Preparation of superhydrophobic polybenzoxazine/SiO_2 films with self-cleaning and ice delay properties, Prog. Org. Coat. 123 (2018) 254–260.
[13] J. Lv, C. Zhu, H. Qiu, J. Zhang, C. Gu, J. Feng, Robust icephobic epoxy coating using maleic anhydride as a crosslinking agent, Prog. Org. Coat. 142 (2020) 105561.
[14] U. Eduok, J. Szpunar, Bioinspired and hydrophobic alkyl-silanized protective polymer coating for Mg alloy, Prog. Nat. Sci.-Mater. 28 (2018) 354–362.
[15] Z. Liu, Z. He, J. Lv, Y. Jin, S. Wu, G. Liu, F. Zhou, J. Wang, Ion-specific ice propagation behavior on polyelectrolyte brush surfaces, RSC Adv. 7 (2017) 840–844.
[16] B. Liang, G. Zhang, Z. Zhong, Y. Huang, Z. Su, Superhydrophilic anti-icing coatings based on polyzwitterion brushes, Langmuir 35 (2019) 1294–1301.
[17] S. Chernyy, M. Järn, K. Shimizu, A. Swerin, S.U. Pedersen, K. Daasbjerg, L. Makkonen, P. Claesson, J. Iruthayaraj, Superhydrophilic polyelectrolyte brush layers with imparted anti-icing properties: effect of counter ions, ACS Appl. Mater. Interfaces 6 (2014) 6487–6496.
[18] D. Chen, M.D. Gelenter, M. Hong, R.E. Cohen, G.H. McKinley, Icephobic surfaces induced by interfacial nonfrozen water, ACS Appl. Mater. Interfaces 9 (2017) 4202–4214.
[19] J. Chen, Z. Luo, Q. Fan, J. Lv, J. Wang, Anti-ice coating inspired by ice skating, Small 10 (2014) 4693–4699.
[20] J. Chen, R. Dou, D. Cui, Q. Zhang, Y. Zhang, F. Xu, X. Zhou, J. Wang, Y. Song, L. Jiang, Robust prototypical anti-icing coatings with a self-lubricating liquid water layer between ice and substrate, ACS Appl. Mater. Interfaces 5 (2013) 4026–4030.
[21] Z. Zhu, J. Xiang, J. Wang, D. Qiu, Effect of polyvinyl alcohol on ice formation in the presence of a liquid/solid interface, Langmuir 33 (2017) 191–196.
[22] F. Wang, S. Xiao, Y. Zhuo, W. Ding, J. He, Z. Zhang, Liquid layer generators for excellent icephobicity at extremely low temperatures, Mater. Horizons 6 (2019) 2063–2072.
[23] G. Zhang, Q. Zhang, T. Cheng, X. Zhan, F. Chen, Polyols-infused slippery surfaces based on magnetic Fe_3O_4-functionalized polymer hybrids for enhanced multi-functional anti-icing and deicing properties, Langmuir 34 (2018) 4052–4058.
[24] C. Tao, S. Bai, X. Li, C. Li, L. Ren, Y. Zhao, X. Yuan, Formation of zwitterionic coatings with an aqueous lubricating layer for antifogging/anti-icing applications, Prog. Org. Coat. 115 (2018) 56–64.
[25] V. Upadhyay, T. Galhenage, D. Battocchi, D. Webster, Amphiphilic icephobic coatings, Prog. Org. Coat. 112 (2017) 191–199.
[26] T.-S. Wong, S.H. Kang, S.K.Y. Tang, E.J. Smythe, B.D. Hatton, A. Grinthal, J. Aizenberg, Bioinspired self-repairing slippery surfaces with pressure-stable omniphobicity, Nature 477 (2011) 443–447.
[27] P. Kim, T.-S. Wong, J. Alvarenga, M.J. Kreder, W.E. Adorno-Martinez, J. Aizenberg, Liquid-infused nanostructured surfaces with extreme anti-ice and anti-frost performance, ACS Nano 6 (2012) 6569–6577.
[28] C. Tao, X. Li, B. Liu, K. Zhang, Y. Zhao, K. Zhu, X. Yuan, Highly icephobic properties on slippery surfaces formed from polysiloxane and fluorinated POSS, Prog. Org. Coat. 103 (2017) 48–59.
[29] Y. Zhuo, F. Wang, S. Xiao, J. He, Z. Zhang, One-step fabrication of bioinspired lubricant-regenerable icephobic slippery liquid-infused porous surfaces, ACS Omega 3 (2018) 10139–10144.
[30] F. Wang, W. Ding, J. He, Z. Zhang, Phase transition enabled durable anti-icing surfaces and its DIY design, Chem. Eng. J. 360 (2019) 243–249.
[31] Y. Zhuo, V. Hakonsen, Z. He, S. Xiao, J. He, Z. Zhang, Enhancing the mechanical durability of icephobic surfaces by introducing autonomous self-healing function, ACS Appl. Mater. Interfaces 10 (2018) 11972–11978.
[32] D.L. Beemer, W. Wang, A.K. Kota, Durable gels with ultra-low adhesion to ice, J. Mater. Chem. A 4 (2016) 18253–18258.
[33] C. Urata, G.J. Dunderdale, M.W. England, A. Hozumi, Self-lubricating organogels (SLUGs) with exceptional syneresis-induced anti-sticking properties against viscous emulsions and ices, J. Mater. Chem. A 3 (2015) 12626–12630.
[34] Y. Wang, X. Yao, J. Chen, Z. He, J. Liu, Q. Li, J. Wang, L. Jiang, Organogel as durable anti-icing coatings, Sci. China Mater. 58 (2015) 559–565.
[35] Y. Zhuo, T. Li, F. Wang, V. Håkonsen, S. Xiao, J. He, Z. Zhang, Ultra-durable icephobic coating by molecular pulley, Soft Matter 15 (2019) 3607–3611.
[36] K. Zhang, X. Li, Y. Zhao, K. Zhu, Y. Li, C. Tao, X. Yuan, UV-curable POSS-fluorinated methacrylate diblock copolymers for icephobic coatings, Prog. Org. Coat. 93 (2016) 87–96.
[37] E.J.Y. Ling, V. Uong, J.-S. Renault-Crispo, A.-M. Kietzig, P. Servio, Reducing ice adhesion on nonsmooth metallic surfaces: wettability and topography effects, ACS Appl. Mater. Interfaces 8 (2016) 8789–8800.
[38] T.K. Chen, Q. Cong, Y. Li, J.F. Jin, K.L. Choy, Utilizing swelling force to decrease the ice adhesion strength, Cold Reg. Sci. Technol. 146 (2018) 122–126.
[39] K. Golovin, S.P. Kobaku, D.H. Lee, E.T. DiLoreto, J.M. Mabry, A. Tuteja, Designing durable icephobic surfaces, Sci. Adv. 2 (2016) e1501496.
[40] K. Golovin, A. Tuteja, A predictive framework for the design and fabrication of icephobic polymers, Sci. Adv. 3 (2017) e1701617.
[41] L. Wang, Q. Gong, S. Zhan, L. Jiang, Y. Zheng, Robust anti-icing performance of a flexible superhydrophobic surface, Adv. Mater. 28 (2016) 7729–7735.
[42] U. Eduok, O. Faye, J. Szpunar, Recent developments and applications of protective silicone coatings: a review of PDMS functional materials, Prog. Org. Coat. 111 (2017) 124–163.
[43] R. Rosenberg, Why is ice slippery? Phys. Today 58 (2005) 50–54.
[44] S. Xiao, J. He, Z. Zhang, Nanoscale deicing by molecular dynamics simulation, Nanoscale 8 (2016) 14625–14632.
[45] J. Chen, K. Li, S. Wu, J. Liu, K. Liu, Q. Fan, Durable anti-icing coatings based on self-sustainable lubricating layer, ACS Omega 2 (2017) 2047–2054.
[46] S. Ozbay, C. Yuceel, H.Y. Erbil, Improved icephobic properties on surfaces with a hydrophilic lubricating liquid, ACS Appl. Mater. Interfaces 7 (2015) 22067–22077.
[47] C. Li, X. Li, C. Tao, L. Ren, Y. Zhao, S. Bai, X. Yuan, Amphiphilic antifogging/anti-icing coatings containing POSS-PDMAEMA-b-PSBMA, ACS Appl. Mater. Interfaces 9 (2017) 22959–22969.
[48] R. Dou, J. Chen, Y. Zhang, X. Wang, D. Cui, Y. Song, L. Jiang, J. Wang, Anti-icing coating with an aqueous lubricating layer, ACS Appl. Mater. Interfaces 6 (2014) 6998–7003.
[49] M. Nosonovsky, V. Hejazi, Why superhydrophobic surfaces are not always icephobic, ACS Nano 6 (2012) 8488–8491.
[50] S. Hwang, C.-H. Choi, C.-S. Lee, Regioselective surface modification of PDMS microfluidic device for the generation of monodisperse double emulsions, Macromol. Res. 20 (2012) 422–428.
[51] V. Sharma, M. Dhayal, Govind, S.M. Shivaprasad, S.C. Jain, Surface characterization of plasma-treated and PEG-grafted PDMS for micro fluidic applications, Vacuum 81 (2007) 1094–1100.
[52] D.K. Sarkar, R.W. Paynter, One-step deposition process to obtain nanostructured superhydrophobic thin films by galvanic exchange reactions, J. Adhes. Sci. Technol.

24 (2010) 1181–1189.
[53] Z. Cheng, S.-H. Teoh, Surface modification of ultra thin poly (ε-caprolactone) films using acrylic acid and collagen, Biomaterials 25 (2004) 1991–2001.
[54] A. Dotan, H. Dodiuk, C. Laforte, S. Kenig, The relationship between water wetting and ice adhesion, J. Adhes. Sci. Technol. 23 (2009) 1907–1915.
[55] D.K. Sarkar, M. Farzaneh, Superhydrophobic coatings with reduced ice adhesion, J. Adhes. Sci. Technol. 23 (2009) 1215–1237.
[56] K. Rykaczewski, S. Anand, S.B. Subramanyam, K.K. Varanasi, Mechanism of frost formation on lubricant-impregnated surfaces, Langmuir 29 (2013) 5230–5238.